Phys. Lett. B 853 (2024) 138674

Contents lists available at ScienceDirect

Physics Letters B

journal homepage: www.elsevier.com/locate/physletb

Letter

# A novel algorithm to the shell model study of heavy deformed nuclei using the variation after projection approach

Zhan-Jiang Lian (连占江) *, Zao-Chun Gao (高早春), Yong-Shou Chen (陈永寿)

*China Institute of Atomic Energy, P.O. Box 275 (10), Beijing 102413, China*

ARTICLE INFO

Editor: A. Schwenk

*Keywords:*
Variation after projection
Shell model
Heavy nuclei

ABSTRACT

We introduce an extension to the conventional variation after projection (VAP) method, in which wave functions of different spin states projected from a shared intrinsic wave function are first varied simultaneously. Then a second variation is carried out for each individual state starting from the obtained intrinsic wave function. This novel algorithm enables the efficient extraction of a rotational band from chaotic non-rotational states by adopting only one Slater determinant, which can not be reached by the conventional VAP method. Some examples including the heavy deformed nuclei in the $jj56$ model space have been calculated. The calculated results show that this new method could be a useful tool to systematically study the collective rotational states in heavy deformed nuclei. Furthermore, the present method holds potential for probing significant correlations, such as octupole correlations, within nuclear structures.

## 1. Introduction

The shell model (SM) is one of the most powerful methods in nuclear physics, which has been proved very successful in describing the ground and low-lying excited states of nuclei. However, as the nuclear system expands, the full SM calculations face a significant challenge due to the exponential increase in dimensionality. To tackle the problem, it is crucial to seek good truncation schemes in a SM study of heavy nuclear systems, which capture the most pertinent configurations. In this way, the basis dimension can be significantly reduced, so that the shell model diagonalization can be performed on contemporary computing platforms. Various approximated SM methods [1–7] with different truncation of the SM space have been developed along this line. These approximated SM methods have greatly extended the shell-model capacity and seem to be applicable over the nuclear chart from the lightest nuclear systems to the superheavy $^{254}$No nucleus [7].

Among them, the variation after projection (VAP) methods are the most elaborated and complete ones. In VAP methods, the broken symmetries in mean-field calculations are restored through the projection techniques and the impact of the projection on the intrinsic wave functions is self-consistently considered. This renders the final VAP wave functions closer to exact SM solutions compared to the mean-field and projection after variation approaches. In a recent study [5], it is reported that, calculations for states of $^{132}$Ba using the VAP method with a single Slater determinant (SD) yielded lower energy than the energy obtained with 50 SDs in the well-known Monte Carlo shell model method [2]. Nevertheless, the complexity of the VAP methods makes the required numerical calculations quite heavy. This historically posed challenges on their application in description of heavy nuclei.

Fortunately, recent advancements in computation power have made VAP calculations for heavy nuclei increasingly feasible. Recently, some successful attempts have been made to calculate the yrast states and few low-lying nonyrast states [5,7]. Yet, challenges persist for higher nonyrast states, as the conventional VAP approaches require calculating all lower states with the same quantum numbers before obtaining the desired state. Such process quickly gets rather complicated as the order of the calculated nonyrast state increases. Thus a systematic application is still difficult if not impossible. To overcome this obstacle, a simple algorithm enabling the straightforward acquisition of high-lying nonyrast states should be developed, so that the high-lying nonyrast states can be obtained as easy as the yrast one.

In this paper, we propose such an algorithm based on the collective nature of heavy deformed nuclei. In the new algorithm, the conventional one-step variation is decomposed into two steps. We first vary the projected wave functions with different spin numbers simultaneously by adopting the same intrinsic wave function. Then starting from the ob-

* Corresponding author.
*E-mail address:* lianzhanjiang@cnncmail.cn (Z.-J. Lian).

https://doi.org/10.1016/j.physletb.2024.138674
Received 14 February 2024; Received in revised form 22 April 2024; Accepted 23 April 2024
Available online 25 April 2024

tained intrinsic wave function, a second variation is carried out for each state. This novel approach permits direct access to nonyrast states without the necessity of calculating lower states. This advancement opens up new possibilities for the systematic and efficient investigation of the collective nuclear motion in heavy nuclei from the SM perspective, which is a long-term pursuit in nuclear physics.

The paper is organized as follows. Section 2 gives an introduction of the proposed algorithm. Section 3 is devoted to a preliminary application of the present method to study rotational bands. A brief summary and outlook is presented in Sec. 4.

## 2. The variation after projection method for rotational bands

Let us start with a brief review of our previous VAP method. Considering the symmetries of rotation and reflection, a nuclear wave function should have good spin and parity. This can be ensured by adopting the techniques of angular-momentum projection and parity projection. With this techniques, the nuclear wave function can be constructed in the following form,

$$|\Psi^{(n)}_{J\pi M\alpha}\rangle = \sum_{i=1}^{n}\sum_{K=-J}^{J} f^{J\alpha}_{Ki} P^{J}_{MK} P^{\pi}|\Phi_i\rangle, \tag{1}$$

where, $P^{J}_{MK}$, $P^{\pi}$ are the projection operators of angular momentum ($J$) and parity ($\pi$), respectively. $\alpha$ is used to label the states with the same $J$, $M$ and $\pi$. Here $|\Phi_i\rangle$ is assumed to be a fully symmetry-unrestricted particle number conserving deformed SD. So the particle number projection is omitted. $n$ is the number of adopted $|\Phi_i\rangle$ basis states.

In principle, with given spin, $J$, and parity, $\pi$, one can get $(2J+1)$ projected states, $P^{J}_{MK}P^{\pi}|\Phi_i\rangle$, for each $|\Phi_i\rangle$ with $K=-J,-J+1,\cdots,J$. All these $(2J+1)$ projected states should be included as in Eq. (1). However, during the optimization process, we found out that the summation of $K$ can be safely removed without sacrificing accuracy [8]. For each $|\Phi_i\rangle$, it is sufficient to select only one of its $(2J+1)$ projected states to construct a normalized VAP wave function, i.e.,

$$|\Psi^{(n)}_{J\pi M\alpha}(K)\rangle = \sum_{i=1}^{n} f^{J\alpha}_{i} P^{J}_{MK} P^{\pi}|\Phi_i\rangle. \tag{2}$$

Here, $K$ can be randomly chosen from the $2J+1$ possible values. All subsequent VAP calculations are performed using wave functions in the form of Eq. (2) with $K=0$.

Given a set of $|\Phi_i\rangle$, the coefficients, $f^{J\alpha}_{i}$, in Eq. (2) and the corresponding energy, $E^{n}_{J\pi\alpha}$, are determined by solving the Hill-Wheeler equation,

$$\sum_{i'}\langle\Phi_i|(\hat{H}-E^{n}_{J\pi\alpha})P^{J}_{KK}P^{\pi}|\Phi_{i'}\rangle f^{J\alpha}_{i'} = 0. \tag{3}$$

Obviously, $E^{n}_{J\pi\alpha}$ is a function of $|\Phi_i\rangle$. According to the variational principle [9], one can keep changing $|\Phi_i\rangle$ until $E^{n}_{J\pi\alpha}$ reaches a minimum. Then the obtained $|\Psi^{(n)}_{J\pi M\alpha}(K)\rangle$ states will be reasonable approximations to the corresponding SM wave functions. This is the normal VAP method that we have adopted in our previous works [8,10].

In the normal VAP method, to calculate the $m$-th state with given $J$ and $\pi$, the number of SDs $n$ should be no less than $m$ [11]. Since the computation time is proportional to $n(n+1)/2$, it is much more time-consuming to calculate the nonyrast state than the yrast one. For instance, the computation time of the fifth nonyrast state is at least 15 times as large as that of the yrast one. This limitation great hinders the application of the normal VAP method in a systematic study of heavy nuclei.

Here we make an extension of the normal VAP method for the study of heavy nuclei by exploiting their collective nature. It is well known that most heavy nuclei are deformed, which is manifested by the appearance of rotational bands. In general, states within the same rotational band share similar intrinsic structures. Considering this fact, we assume the wave functions of states within a rotational band can be projected from the same intrinsic wave function. In the present work, only one SD, $|\Phi\rangle$, is considered. Then, the corresponding VAP wave function for each state can be expressed as

$$|\Psi_{J\pi M}(K)\rangle = \frac{P^{J}_{MK}P^{\pi}|\Phi\rangle}{\sqrt{\langle\Phi|P^{J}_{KK}P^{\pi}|\Phi\rangle}}. \tag{4}$$

Here $K$ represents the magnetic quantum number associated with the calculated band. Varying the SD, $|\Phi\rangle$, all the corresponding $|\Psi_{J\pi M}(K)\rangle$ states and their energies, $E_{J\pi}$, should change accordingly. The key is how to determine the optimized $|\Phi\rangle$. In Ref. [11], we have proved that, for a state with quantum number $J$, $\pi$ and $\alpha$, its VAP energy $E^{n}_{J\pi\alpha}$ obtained from Eq. (3) is always no less than the corresponding SM energy $E^{\mathrm{SM}}_{J\pi\alpha}$, i.e.,

$$E^{n}_{J\pi\alpha} \geq E^{\mathrm{SM}}_{J\pi\alpha}. \tag{5}$$

Here we define the non-negative energy differences $\delta E_{J\pi} = E_{J\pi} - E^{\mathrm{SM}}_{J\pi}$ and the total energy difference

$$\Delta E = \sum_{J}\delta E_{J\pi} = \sum_{J} E_{J\pi} - \sum_{J} E^{\mathrm{SM}}_{J\pi}. \tag{6}$$

It is obvious that the optimized $|\Phi\rangle$ should be the one that $\Delta E$ reaches a minimum. Since $E^{\mathrm{SM}}_{J\pi}$ in Eq. (6) are fixed for a given Hamiltonian, instead of minimizing the $\Delta E$, one can equivalently minimize the sum of the $E_{J\pi}$ energies,

$$S = \sum_{J} E_{J\pi}. \tag{7}$$

Such minimization of $S$ is ensured by the Hylleraas-Undheim-MacDonald (HUM) theorem [12,13], as has been clearly addressed in Ref. [11].

Obviously, when only one $J$ is included in Eq. (7), the obtained state corresponds to the yrast state. As more additional states with different spin are incorporated, more restrictions are provided on the intrinsic wave function in variation. Thus the resulting projected states should exhibit deviations from the yrast ones. It is reasonable to expect a gradual evolution of these projected states from the yrast configuration towards a rotational structure since they are projected from the same SD and share a common intrinsic structure. But it should be mentioned that the minimization of $S$ does not necessarily imply the minimization of each individual $E_{J\pi}$. Thus, to ensure $|\Psi_{J\pi M}(K)\rangle$ is fully optimized, one should further perform a second variation calculation for each state starting from the intrinsic wave function obtained in the previous variation. Here, we call this new algorithm as the variation after projection method for rotational bands (VAP-R) to show the difference from the normal VAP method.

## 3. The numerical results

To show the validity of the present method, we first perform VAP-R calculations for $^{56}$Ni. In $^{56}$Ni, two well deformed rotational bands with opposite parity have been identified from experiment [14]. States within these two bands are all nonyrast and embedded in other chaotic non-rotational states. Here the positive parity band is considered. We set $K=0$ and adopt the GXPF1A interaction [15] in the $pf$ shell model space. The minimized $S$ in Eq. (7) includes those energies with $J^{\pi}=0^{+},2^{+},4^{+},\cdots,J^{+}_{\max}$. $J_{\max}$ is taken as $0,4,8,12,16$, respectively. All calculations with different $J_{\max}$ are performed start from the same randomly selected initial trial wavefunction $|\Phi_0\rangle$, which is constructed in the same way as Ref. [16] through the Thouless theorem,

$$|\Phi_0\rangle = \mathcal{N}_i e^{\frac{1}{2}\sum_{\mu\nu} d^{i}_{\mu\nu} c^{\dagger}_{\mu} c_{\nu}}|\Phi_{00}\rangle, \tag{8}$$

where $|\Phi_{00}\rangle = \prod_{i=1}^{A} c^{\dagger}_{i}|0\rangle$ and $c^{\dagger}_{i}$ denotes the creation operator of the spherical single particle basis $|i\rangle = |Nljm\rangle$. $|\Phi_0\rangle$ is parametrized by the $d^{i}_{\mu\nu}$ matrix elements generated stochastically and can be any other SD, which is not orthogonal to $|\Phi_{00}\rangle$. The optimization problem is solved

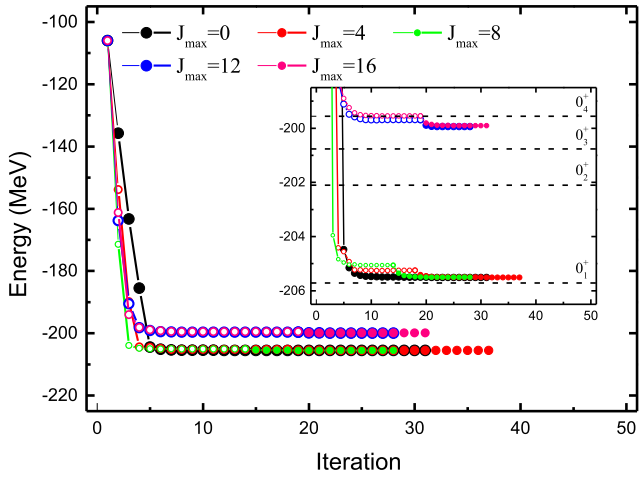


**Fig. 1.** The convergence patterns of the energy of the $J^\pi = 0^+$ state in $^{56}$Ni using VAP-R. The open circle and solid circle denote results in the first and second variation, respectively. The exact SM energies are shown by the dash lines.

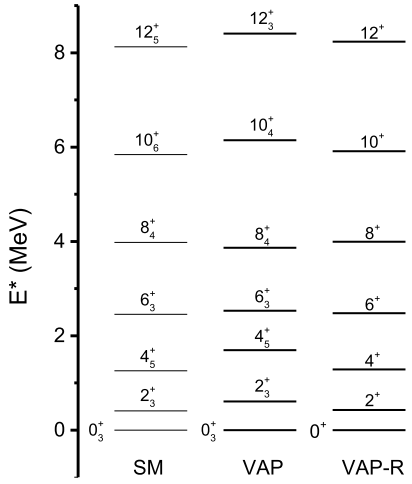


**Fig. 2.** Comparison of the positive parity band in $^{56}$Ni obtained from SM, VAP and VAP-R calculations. The energy of the $J^\pi = 0^+$ bandhead is set to 0.

using the trust region algorithm [17] (more detail can be found in Ref. [16]). To avoid the appearance of vanishing overlaps in solving the HW equation, an additional constraint term proposed in Ref. [18] has been attached to the energy sum. The final minimized quantity is,

$$S' = S + \chi \sum_J \frac{1}{\langle \Phi | P^J_{KK} P^\pi | \Phi \rangle}, \tag{9}$$

where $\chi$ is a tiny number equal to $10^{-4}$.

Fig. 1 shows the convergence patterns of the energy of the $J^\pi = 0^+$ state with different $J_{\max}$. For comparison, the exact shell model energies are also calculated using the NUSHELLX code [19], which are represented by the dash lines. One can see that the final obtained $J^\pi = 0^+$ state corresponds to the yrast state as usual when $J_{\max} \leq 8$. As more additional states are added to the summation, however, the result becomes quite different. As expected, it suddenly changes from the $0^+_1$ state to the $0^+_3$ state, which is theoretically identified as the bandhead of the positive parity rotational band [20].

Fig. 2 further compares the whole positive parity band in $^{56}$Ni obtained from the SM method, the normal VAP method and the VAP-R method. The SM calculation shows the $J^\pi = 10^+$ state within the rotational band has the highest order of 6 [20]. To ensure all the states within the band can be obtained, 8 SDs are used in the normal VAP calculations. For each spin $J$, the normal VAP variational calculations are

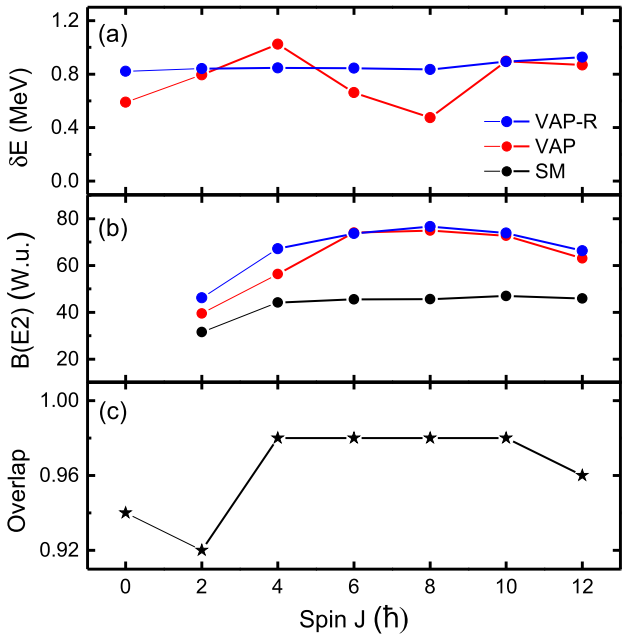


**Fig. 3.** (a) Energy differences between the SM energies and the normal VAP (red dots) and the VAP-R (blue dots) energies of states in the positive parity band in $^{56}$Ni; (b) The $B(E2; J \to J-2)$ values between states in band. The effective charges $(e_p, e_n) = (1.5, 0.5)e$. (c) The values of the overlap, $|\langle \Psi^{\rm VAP}_{J\pi M}(K) | \Psi^{\rm VAP-R}_{J\pi M}(K) \rangle|$.

performed so that the summation of the lowest 6 energy expectation values is minimized [11]. In the SM and the normal VAP calculations, the states in the band are identified by the large $B(E2; J \to J-2)$ values between band members (see Fig. 3(b)). The VAP-R results are obtained by taking $J_{\max} = 12$. One can see that the SM band structure has been well reproduced by both the normal VAP and the VAP-R calculations. More interestingly, although only one SD is adopted, both the energies and the $B(E2)$ values obtained from the VAP-R calculations are very close to the normal VAP results. Actually, as can be seen from Fig. 3(c), most of the calculated overlaps, $|\langle \Psi^{\rm VAP}_{J\pi M}(K) | \Psi^{\rm VAP-R}_{J\pi M}(K) \rangle|$, between the wave functions obtained from VAP-R and VAP are above 0.96. However, for each spin state, there still exists an energy difference of about 0.8-0.9 MeV between the VAP-R energy and the SM one due to the truncation of the configuration space (see Fig. 3(a)). This also results in some discrepancy in the $B(E2)$ values. As in the case of other approximated SM methods, such difference can be reduced by adopting more SDs in the VAP-R calculations. The VAP-R calculations with multireference states will be explored in the future.

To demonstrate the important applicability of the present method to heavy deformed nuclei, the ground-state band ($K^\pi = 0^+$) and the $\gamma$-vibration band ($K^\pi = 2^+$) of the rare-earth nucleus $^{160}$Dy are calculated in the $jj56$ model space. The $jj56$ shell model space consists of all single-particle orbits between the shell closures of $^{132}$Sn and $^{208}$Pb. The $m$-scheme dimension of $^{160}$Dy is $4.4 \times 10^{17}$, which is roughly $10^6$ times larger than the current limitation of the conventional Lanczos method. Here the jj56pnb interaction is adopted. As described in Ref. [21,22], the proton-proton interactions were based on the CD Bonn potential. The interactions for the proton-neutron space and the neutron-neutron space were obtained from the $N^3LO$ potential. Fig. 4 compares the experimental data with the calculated results using the VAP-R method and the normal VAP method. In VAP-R calculations of the ground-state band, $K$ is set to 0 and the positive parity even-spin states with $J$ up to 20 are all included in the summation. For the $\gamma$-vibration band, we set $K = 2$ and the included spins are $J^\pi = 0^+, 1^+, 2^+, \cdots, 10^+, 11^+$. For each spin $J$, the normal VAP calculation is performed by minimizing the lowest 3 energy expectation values using 4 SDs. Then the two bands

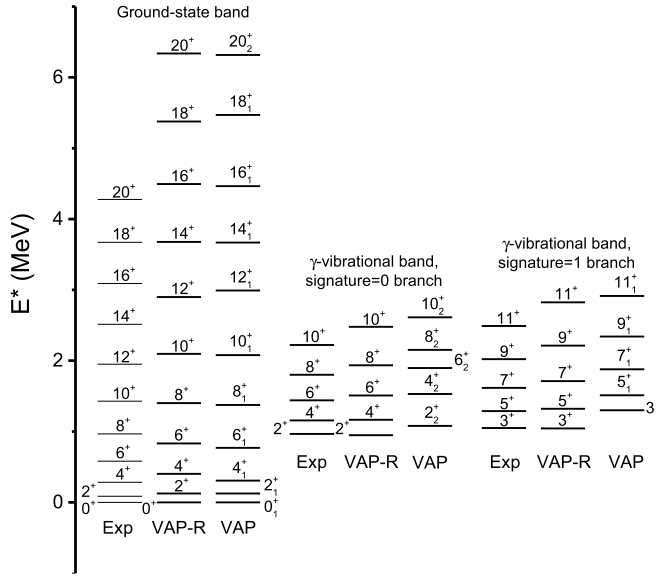


**Fig. 4.** Comparison of excitation energies among the experimental data, the VAP-R results and the normal VAP results for $^{160}$Dy. The experimental data is taken from Ref. [23].

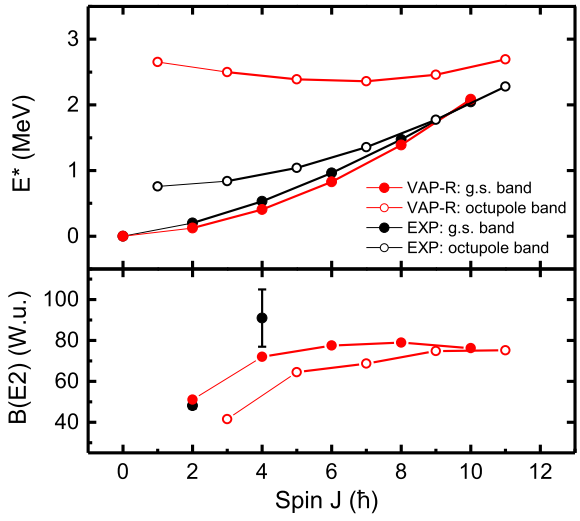


**Fig. 5.** Comparison of (a) excitation energies and (b) the intra-band $B(E2; J \rightarrow J-2)$ values between the experimental data (black symbols) and the VAP-R results (red symbols) for $^{144}$Ba. The effective charges $(e_p, e_n) = (1.5, 0.5)e$ and the experimental data is taken from Ref. [23].

are identified by the large intra-band $B(E2)$ values. It is shown that the VAP-R results are very close to the VAP ones for both bands. Most of the calculated overlaps between the wave functions are above 0.95. Interestingly, as compare to the VAP results, the $2^+$ state bandhead and the even-odd staggering of the $\gamma$-vibration band are much better reproduced in VAP-R calculations and the calculated results show an excellent agreement with the experimental data. This may be due to the better incorporation of the collective nuclear motion in determining the VAP-R intrinsic wave functions. Nevertheless, the calculated moments of inertia of both bands are smaller than the experimental ones. This indicates that the necessary modification of the present jj56pnb interaction, as done in the *sd* and *pf* shell [15,24], perhaps be required for a better description of the nuclear properties in this mass region.

From above discussions, one can see that, in the normal VAP method, a certain number of SDs should be used to describe a rotational band with nonyrast states. However, VAP-R calculations are capable to reproduce such band by adopting only one SD. The calculated results are very close to the normal VAP ones and the collective nuclear motion seems to be better described. Since the computation time is proportional to $n(n+1)/2$, the computational cost of the VAP-R calculations is obviously much lower than that of the normal VAP calculations. On the other hand, one can understand that the less number of SDs are adopted, the faster the convergence speed is. Actually, for most calculated states in above examples, the VAP-R calculations converge about 1-2 times faster than the corresponding VAP calculations. Compared to the normal VAP method, the VAP-R method, on the whole, can reduce the computation time by up to two orders of magnitude in calculation of nonyrast states of a high order. Considering the fact even the one-SD VAP calculation for heavy nuclei already requires a large amount of computation time ($1-2$ days for a complete iteration of a single state of $^{160}$Dy on an Nvidia Tesla V100 GPU), the present improvement is of great importance to a systematic SM study of the collective properties of heavy nuclei, especially for abundant high excited bands.

Now we introduce another advantage of the present method. We find that, other than one single band, the VAP-R method is able to reproduce multi rotational bands simultaneously in one calculation as long as they have a similar intrinsic structure. This nice feature may provide us a simple way to explore some important correlations in nuclei, such as the octupole correlation and the tetrahedral symmetry, which are manifested by the appearance of two or more rotational bands.

To show this, here we take $^{144}$Ba as an example. Theoretical and experimental evidence [25–27] shows that there exist strong octupole correlations in the neutron-rich nucleus $^{144}$Ba, giving rise to a low-lying negative parity octupole band above the positive parity ground state band. To study them within the SM framework, we set $K = 0$ and perform a VAP-R calculation for $^{144}$Ba by including $J^\pi = 0^+, 1^-, 2^+, \cdots, 10^+, 11^-$ in the summation. The jj56pnb interaction is adopted and the results are shown in Fig. 5. The large intra-band $B(E2)$ values confirm that two rotational bands have been obtained in our calculation. For the ground state band, both the energies and the $B(E2)$ values obtained from the VAP-R calculation have a good agreement with the experimental results. However, it seems that the energies of the octupole band can not be well reproduced by the present effective interaction, which indicates again the necessary modification of the jj56pnb interaction. As a result, the calculated reduced transition probability $B(E3; 3^- \rightarrow 0^+)$ only has a value of 3.8 W.u., much smaller than the measured value $48(^{+25}_{-34})$ W.u. [27]. But this enhanced value and the similar intrinsic structure of two bands can still give us a hint of the existence of octupole correlations in $^{144}$Ba.

## 4. Summary and outlook

In summary, we have developed a new method called as the VAP-R method, in which the projected wave functions with different spin numbers are first varied simultaneously before performing calculations for each individual state. This method is able to automatically pick out the rotational band from the chaotic non-rotational states by adopting only one SD. Compared to the normal VAP method, the present method, in description of well deformed nuclei, not only can save a lot of computation time, but also do not have a significant loss of approximation. This makes it efficient and promising in a systematic SM study of the collective nuclear properties of heavy deformed nuclei, which was hardly reachable previously. Moreover, the VAP-R method can also serve as a useful tool to reproduce different rotational bands with a similar intrinsic structure and help us explore the underlying correlations in nuclei.

As a preliminary work, only one SD is adopted to ensure the rotational band can be safely extracted. There is some discrepancy between the calculated results and the SM ones. Like in VAP, one may expect the present VAP-R results can be further improved by considering particle-hole expansion or adopting more SDs [28–31]. Such work is in progress.

## Declaration of competing interest

The authors declare that they have no known competing financial interests or personal relationships that could have appeared to influence the work reported in this paper.

## Data availability

Data will be made available on request.

## Acknowledgements

This work is supported by Continuous-Support Basic Scientific Research Project, by the Key Laboratory of Nuclear Data foundation (JCKY2022201C158), by YZ232604001601 and by the National Natural Science Foundation of China under Grant No. 11975314.

## References

[1] M. Horoi, B.A. Brown, V. Zelevinsky, Phys. Rev. C 50 (1994) R2274.
[2] T. Otsuka, M. Honma, T. Mizusaki, N. Shimizu, Y. Utsuno, Prog. Part. Nucl. Phys. 47 (2001) 319.
[3] Z.C. Gao, M. Horoi, Y.S. Chen, Phys. Rev. C 92 (2015) 064310.
[4] K.W. Schmid, Prog. Part. Nucl. Phys. 52 (2004) 565.
[5] N. Shimizu, Y. Tsunoda, Y. Utsuno, T. Otsuka, Phys. Rev. C 103 (2021) 014312.
[6] B. Bally, A. Sánchez-Fernández, T.R. Rodríguez, Eur. Phys. J. A 57 (2021) 69.
[7] D.D. Dao, F. Nowacki, Phys. Rev. C 105 (2022) 054314.
[8] Zao-Chun Gao, Phys. Lett. B 824 (2022) 136795.
[9] P. Ring, P. Schuck, The Nuclear Many-Body Problem, Springer Verlag, New York/Heidelberg/Berlin, 1980.
[10] Zhan-Jiang Lian, Xiao Lu, Zao-Chun Gao, Phys. Rev. C 106 (2022) 044308.
[11] Jia-Qi Wang, Zao-Chun Gao, Ying-Jun Ma, Y.S. Chen, Phys. Rev. C 98 (2018) 021301(R).
[12] E.A. Hylleraas, B. Undheim, Z. Phys. 65 (1930) 759.
[13] J.K.L. MacDonald, Phys. Rev. 43 (1933) 830.
[14] D. Rudolph, C. Baktash, M.J. Brinkman, E. Caurier, D.J. Dean, M. Devlin, J. Dobaczewski, et al., Phys. Rev. Lett. 82 (1999) 3763.
[15] M. Honma, T. Otsuka, B.A. Brown, T. Mizusaki, Eur. Phys. J. A 25 (Suppl. 1) (2005) 499.
[16] T. Ya, Y. He, Z.-C. Gao, J.-Q. Wang, Y.S. Chen, Phys. Rev. C 95 (2017) 064307.
[17] J. Norcedal, S.J. Wright, Numerical Optimization, Springer Verlag, New York/Berlin/Heidelberg, 2006.
[18] Xiao Lu, Zhan-jiang Lian, Xue-wei Li, Zao-chun Gao, Yong-shou Chen, Chin. Phys. C 47 (2023) 074104.
[19] B.A. Brown, W.D.M. Rae, E. McDonald, M. Horoi, NuShellX@MSU, http://www.nscl.msu.edu/~brown/resources/resources.html;
W.D.M. Rae, NuShellX, http://www.garsington.eclipse.co.uk/.
[20] M. Horoi, B.A. Brown, T. Otsuka, M. Honma, T. Mizusaki, Phys. Rev. C 73 (2006) 061305(R).
[21] B.A. Brown, N.J. Stone, J.R. Stone, I.S. Towner, M. Hjorth-Jensen, Phys. Rev. C 71 (2005) 044317.
[22] J.M. Allmond, A.E. Stuchbery, B.A. Brown, J.R. Beene, A. Galindo-Uribarri, C.J. Gross, et al., Phys. Rev. C 90 (2014) 014322.
[23] Brookhaven database, http://www.nndc.bnl.gov.
[24] B.A. Brown, W.A. Richter, Phys. Rev. C 74 (2006) 034315.
[25] L.M. Robledo, M. Baldo, P. Schuck, X. Vias, Phys. Rev. C 81 (2010) 034315.
[26] K. Nomura, D. Vretenar, T. Niki, B.-N. Lu, Phys. Rev. C 89 (2014) 024312.
[27] B. Bucher, S. Zhu, C.Y. Wu, R.V.F. Janssens, D. Cline, et al., Phys. Rev. Lett. 116 (2016) 112503.
[28] P.W. Zhao, P. Ring, J. Meng, Phys. Rev. C 94 (2016) 041301(R).
[29] J. Ripoche, T. Duguet, J.-P. Ebran, D. Lacroix, Phys. Rev. C 97 (2018) 064316.
[30] M. Frosini, T. Duguet, J.-P. Ebran, V. Somà, Eur. Phys. J. A 58 (2022) 62.
[31] Xiao Lu, Zhan-jiang Lian, Zao-chun Gao, Phys. Rev. C 107 (2023) 054313.